Neurotoxicology 71 (2019) 39–51

Contents lists available at ScienceDirect

Neurotoxicology

journal homepage: www.elsevier.com/locate/neuro

Full Length Article

# Alpha-naphthoflavone induces apoptosis through endoplasmic reticulum stress via c-Src-, ROS-, MAPKs-, and arylhydrocarbon receptor-dependent pathways in HT22 hippocampal neuronal cells

Ah-Ran Yu[a], Yeon Ju Jeong[a], Chi Yeon Hwang[a], Kyung-Sik Yoon[a,b], Wonchae Choe[a,b], Joohun Ha[a,b], Sung Soo Kim[a,b], Youngmi Kim Pak[c], Eui-Ju Yeo[d,**], Insug Kang[a,b,*]

[a] Department of Biomedical Sciences, Graduate School, Kyung Hee University, Seoul, 02447, Republic of Korea
[b] Department of Biochemistry and Molecular Biology, School of Medicine, Biomedical Science Institute, Kyung Hee University, Seoul, 02447, Republic of Korea
[c] Department of Physiology, School of Medicine, Biomedical Science Institute, Kyung Hee University, Seoul, 02447, Republic of Korea
[d] Department of Biochemistry, College of Medicine, Gachon University, Incheon, 21999, Republic of Korea

ARTICLE INFO

*Keywords:*
α-Naphthoflavone
Aryl hydrocarbon receptor modulator
Apoptosis
ER stress
HT22 hippocampal neuronal cells

ABSTRACT

α-Naphthoflavone (αNF) is a prototype flavone, also known as a modulator of aryl hydrocarbon receptor (AhR). In the present study, we investigated the molecular mechanisms of αNF-induced cytotoxic effects in HT22 mouse hippocampal neuronal cells. αNF induced apoptotic cell death via activation of caspase-12 and -3 and increased expression of endoplasmic reticulum (ER) stress-associated proteins, including C/EBP homologous protein (CHOP). Inhibition of ER stress by treatment with the ER stress inhibitor, salubrinal, or by CHOP siRNA transfection reduced αNF-induced cell death. αNF activated mitogen-activated protein kinases (MAPKs), such as p38, JNK, and ERK, and inhibition of MAPKs reduced αNF-induced CHOP expression and cell death. αNF also induced accumulation of reactive oxygen species (ROS) and an antioxidant, N-acetylcysteine, reduced αNF-induced MAPK phosphorylation, CHOP expression, and cell death. Furthermore, αNF activated c-Src kinase, and inhibition of c-Src by a kinase inhibitor, SU6656, or siRNA transfection reduced αNF-induced ROS accumulation, MAPK activation, CHOP expression, and cell death. Inhibition of AhR by an AhR antagonist, CH223191, and siRNA transfection of AhR and AhR nuclear translocator reduced αNF-induced AhR-responsive luciferase activity, CHOP expression, and cell death. Finally, we found that inhibition of c-Src and MAPKs reduced αNF-induced transcriptional activity of AhR. Taken together, these findings suggest that αNF induces apoptosis through ER stress via c-Src-, ROS-, MAPKs-, and AhR-dependent pathways in HT22 cells.

## 1. Introduction

Environmental pollutants, such as dioxins and polycyclic aromatic hydrocarbons, and polychlorinated biphenyls, can cause acute and chronic toxicity, including chloracne, immune suppression, inflammation, reduced fertility, hepatotoxicity, tumor promotion, and cell death (Chepelev et al., 2015; Chopra and Schrenk, 2011; Furness and Whelan, 2009; Kakeyama and Tohyama, 2003). These compounds induce the expression of xenobiotic-metabolizing enzymes, such as cytochrome p450 (CYP)1 A1, CYP1 A2, CYP1B1, and phase II enzymes (Denison and Nagy, 2003; Murray et al., 2014). The induction of these genes occurs via the aryl hydrocarbon receptor (AhR).

The AhR is a ligand-activated transcription factor of the Per-ARNT-Sim (PAS) protein family, possessing a sequence homology domain previously identified in period circadian protein, aryl hydrocarbon receptor nuclear transporter (ARNT), and single-minded protein. The inactive AhR in cytoplasm forms a complex with HSP90 and other scaffold proteins, such as p23 and immunophilin-like AhR-interacting protein. Upon ligand binding, AhR dissociates from the complex, translocates to the nucleus, and heterodimerizes with ARNT. The activated AhR and ARNT complex binds to dioxin or xenobiotic response elements (DREs or XREs) which are located in the enhancer/promoter region of AhR target genes, such as CYP1 A1, CYP1 A2, and CYP1B1 (Murray et al., 2014). Beside its involvement in metabolism of xenobiotics, AhR is shown to play physiological roles in cell proliferation and differentiation, in liver and immune system homeostasis, and in tumor development (Barouki et al., 2007; Opitz et al., 2011). Previously, it has been reported that c-Src tyrosine kinase is associated

* Corresponding author at: Department of Biochemistry and Molecular Biology, School of Medicine, Kyung Hee University, Seoul, 02447, Republic of Korea.
** Corresponding author at: Department of Biochemistry, College of Medicine, Gachon University, Incheon, 21999, Republic of Korea.
*E-mail addresses:* euiju@gachon.ac.kr (E.-J. Yeo), iskang@khu.ac.kr (I. Kang).

https://doi.org/10.1016/j.neuro.2018.11.011
Received 28 August 2018; Received in revised form 20 November 2018; Accepted 22 November 2018
Available online 30 November 2018
0161-813X/ 

with the AhR complex, activated by dioxin, and mediates AhR signaling (Backlund and Ingelman-Sundberg, 2005; Dong and Matsumura, 2009; Matsumura, 2009; Tomkiewicz et al., 2013; Xie et al., 2012). The roles of c-Src and downstream signaling pathways in the AhR responses are not clarified yet. It is also known that AhR and its target genes are expressed in many tissues including the brain and AhR activation by ligands induces acute brain damage and apoptotic neuronal cell death (Cuartero et al., 2014; Morales-Hernandez et al., 2016; Williamson et al., 2005). However, the molecular mechanism underlying AhR-mediated neurotoxicity is largely unknown.

α-Naphthoflavone (αNF), a prototype flavone, is also known as 7,8-benzoflavone and is a modulator of AhR with both agonistic and antagonistic actions (Murray et al., 2011; Santostefano et al., 1993). αNF is shown to have various effects, including anti-ageing, anti-platelet properties, vasodilation, and neuroprotection (Cheng et al., 2003; Hsiao et al., 2005; Liao et al., 2012; Zhu et al., 2017). The role of αNF as an anti-cancer agent has also been reported in breast cancer cells (Datta et al., 2015; Mense et al., 2009). Even though αNF was shown to antagonize $H_2O_2$-induced apoptosis in human neuroblastoma SH-SY5Y cells (Zhu et al., 2017) and βNF-induced apoptosis in mouse primary neuronal cells (Kajta et al., 2009), it also exerted pro-apoptotic effects in human cervical cancer HeLa cells in an AhR-independent manner (Flores-Perez and Elizondo, 2018). Therefore, the effect of αNF itself on apoptosis of neuronal cells and its molecular mechanisms remain to be further elucidated.

The endoplasmic reticulum (ER) is a type of membranous organelle, where secretory proteins are folded and processed (Kaufman, 1999). Disturbance in the function or structure of the ER causes ER stress via the accumulation of unfolded proteins in the ER lumen and alteration of $Ca^{2+}$ homeostasis (Boyce and Yuan, 2006). ER stress initially activates specific signaling pathways in a process known as the unfolded protein response. These signaling pathways include three key proteins, such as the PKR-like endoplasmic reticulum kinase (PERK), inositol-requiring enzyme 1 (IRE1), and activating transcription factor 6 (ATF6). The activated PERK phosphorylates eukaryotic initiation factor 2α (eIF2α), resulting in translational inhibition (Boyce et al., 2005). When the ER functions are severely impaired, apoptosis occurs to protect the organism by eliminating damaged cells. C/EBP homologous protein (CHOP) and caspase-12 participate in ER stress-mediated apoptosis (Zinszner et al., 1998). Activation of MAPKs, accumulation of cytosolic ROS and $Ca^{2+}$, and mitochondrial dysfunction are implicated in the upstream signaling pathways for ER stress induction (Choi et al., 2011). Accumulating evidence suggests that ER stress is linked to several neurodegenerative diseases, including Alzheimer's disease, Parkinson disease, and cerebral ischemia (Lindholm et al., 2006).

Therefore, in this study, we investigated which molecular mechanisms are involved in αNF-induced neuronal cell death. We found that αNF induces apoptotic cell death through ER stress via c-Src-, ROS- and MAPKs-, and AhR-dependent pathways in HT22 murine hippocampal neuronal cells.

## 2. Materials and methods

### 2.1. Materials

Dulbescco's modified Eagle's medium (DMEM), fetal bovine serum (FBS), and the other cell culture products were purchased from Life Technologies (Grand Island, NY). 2-phenyl-2,3-dihydro-aH-benzo[*h*]chromen-4-one (αNF), thapsigargin (TG), CH223191, 3-(4,5-dimethylthiazol-e-yl)-2,5-diphenyl tetrazolium (MTT), N-acetylcysteine (NAC), propidium iodide (PI), 2′,7′-dichlorodihydrofluorescein diacetate (DCF-DA), DiOC6, SU6656, 2,3,7,8-tetrachlorodibenzo-p-dioxin (TCDD), small interfering RNAs (siRNAs) for p38α and AhR, and TRI reagent were obtained from Sigma-Aldrich (St. Louis, MO, USA). Annexin V-fluorescein isothiocynate (FITC) apoptosis detection kit was from BD Bioscience (Oakville, Ontario, Canada). Fura-2 AM was obtained from ENZO Life Sciences (Farmingdale, NY, USA). Antibodies against CHOP, eIF2α, p38, JNK, ERK, and c-Src, HRP-conjugated anti-goat and anti-rabbit secondary antibodies were purchased from Santa Cruz Biotechnology (Santa Cruz, CA). Taq polymerase kits, primers for a reverse transcription-polymerase chain reaction (RT-PCR) assay, and siRNAs for scrambled control, CHOP, JNK, ERK, c-Src, and ARNT were purchased from Bioneer (Seoul, Korea). Antibodies against caspase-12, caspase-3, PARP, phospho-eIF2α, phospho-p38, phospho-JNK, phospho-ERK, and phospho-c-Src were obtained from Cell Signaling Technology (Beverly, MA). SB203580, SP600125, and PD98059 were purchased from Tocris (Bristol, UK). Enhanced chemiluminescence (ECL) system was acquired from Amersham (GE Health care, Piscataway, NJ, USA) and GeneSilencer siRNA transfection reagent was obtained from Genlantis (San Diego, CA, USA). Dual-luciferase reporter assay system was obtained from Promega (Fitchburg, WI, USA).

### 2.2. Cell culture

HT22 murine hippocampal neuronal cells were cultured in DMEM supplemented with 10% FBS, 100 U/ml penicillin, and 100 μg/ml streptomycin in a humidified 5% $CO_2$ incubator at 37°C. For the experiments, the HT22 cells were serum-starved for 3 h and incubated with αNF or other drugs. On completion of incubation, cells were washed with phosphate-buffered saline (PBS) and subjected to various analyses.

### 2.3. MTT assay

Cell viability was determined based on the conversion of MTT to MTT-formazan by mitochondrial enzymes as follows. Briefly, cells were seeded into a 12-well plate at a density $2 \times 10^5$ cells/well in 1 ml of medium in triplicate, stabilized to grow, and then treated with various concentrations of αNF or TG. After 24 h of incubation at 37°C, 100 μl MTT solution (5 mg/ml stock) was added to the cells, and they were then incubated for 1 h at 37°C. The medium was removed carefully and then 100 μl dimethyl sulfoxide was added to resolve the blue formazan in living cells. Finally, the absorbance was measured on an ELISA plate reader (Multiskan EX, Thermo Lab system, Beverly, MA, USA) with a test wavelength at 540 nm and with a reference wavelength at 650 nm. The optical density at 650 nm was subtracted from that at 540 nm and then the net values were expressed as the percentage compared to the control.

### 2.4. Western blot analysis

For western blot analysis, HT22 cells ($3 \times 10^5$ cells/well) in 3 ml of medium were incubated for 24 h at 37 °C in a 6-cm culture dish. The cells were then washed twice with ice-cold PBS, and the total cell lysates were prepared in a lysis buffer containing 50 mM Tris − HCl (pH 7.4), 150 mM NaCl, 1% Triton X-100, 50 mM NaF, 5 mM sodium pyrophosphate, 1 mM EDTA, 1 mM EGTA, 1 mM DTT, 0.1 mM PMSF, and 0.5% protease inhibitor cocktail. The whole cell lysates were centrifuged (12,000 × g for 10 min at 4 °C) to remove cellular debris. The protein concentration was determined by the Lowry method using a Bio-Rad DC protein assay kit. Cell lysates containing equal amounts of protein (40 μg) were resolved by 8–15% SDS-polyacrylamide gel electrophoresis and then transferred onto nitrocellulose membranes. The blots were blocked with a solution containing 5% skim milk in Tris-buffered saline with 0.05% Tween 20 (TBST) for 1 h at room temperature, and treated with primary antibodies in TBST overnight at 4 °C. Membranes were washed for 1 h with TBST and further probed with secondary HRP-conjugated anti-rabbit IgG in TBST for 1 h at room temperature. Finally, the immune complexes were visualized using an ECL detection system according to the manufacturer's protocols.

### 2.5. Flow cytometry for DNA content analysis and annexin V-FITC/PI double-staining assay

To detect apoptotic cell death, HT22 cells were seeded at $2 \times 10^5$ cells/ml in a 10-cm culture dish, and treated with 20 μM αNF. After incubation for 24 h, the cells were harvested, washed twice with PBS, and then fixed with ice-cold 75% ethanol at 4 °C for 24 h. The cells were subsequently pelleted by centrifugation at 1000 ×g for 5 min and the ethanol layer was discarded. After washing with PBS, the fixed cells were treated with 0.5 μg/ml RNase A in PI buffer for 30 min. At the end of treatment, the cells were stained with PI (20 μg/ml) for 30 min in the dark. The cell cycle was then analyzed for the DNA contents using the Kaluza flow cytometry software (Beckman Coulter, Orange Country, CA, USA). Apoptotic cell death was also detected by flow cytometry using the annexin V-FITC/PI double-labeling method. After treatment with αNF, HT22 cells were trypsinized and collected by centrifugation. After resuspension in annexin V-FITC binding buffer, the cells were incubated with 1 μg/ml annexin V-FITC and 10 μg/ml PI at room temperature in the dark for 15 min. The samples were analyzed using Kaluza flow cytometry.

### 2.6. RNA interference by siRNA

Transfection of siRNA was conducted using GeneSilencer siRNA transfection reagent. HT22 cells were plated in 6-well plates overnight and the media were replaced with 1 ml of serum-free DMEM before transfection. Scrambled control, CHOP, p38α, JNK, ERK, c-Src, AhR, ARNT siRNA duplexes (100 nM) were incubated with 5 μl of siRNA transfection reagent for 5 min at room temperature; the siRNA mixtures were then added to these cells. After 12 h of incubation with siRNAs in the absence of serum, 1 ml DMEM containing 20% FBS was added to each well and incubated for additional 24 h. Cells were then treated with αNF or TG for 24 h.

### 2.7. Measurement of ROS

To measure the ROS production, cells were treated with 20 μM αNF for the indicated times and then incubated with 10 μM DCF-DA for 1 h. The cells were washed twice with ice-cold PBS, followed by suspension in the same buffer. The fluorescence intensity was measured by flow cytometry (Beckman Coulter) using excitation and emission wavelength of 488 and 525 nm, respectively. Ten thousand events were analyzed per sample.

### 2.8. Assessment of mitochondrial membrane potential (MMP)

To assess MMP loss, cells were treated with 20 μM αNF for 12 h. Cells were washed twice with PBS, resuspended in PBS containing 20 nM DiOC6 and 20 μg/ml PI, and then incubated at 37 °C for 15 min. Fluorescence intensity was examined in cells at channel FL1 for DiOC6 or channel FL3 for PI. Non-apoptotic cells were stained green with DiOC6 and apoptotic cells showed decreased intensity of DiOC6 staining, while necrotic cells were stained red with PI. Fluorescence intensity was then measured by flow cytometry using excitation and emission wavelengths of 482 and 504 nm, respectively. At least twenty thousand events were analyzed per sample and each sample was performed in duplicate.

### 2.9. Measurement of cytosolic $Ca^{2+}$

For the spectrofluorimetric measurements, cells were loaded with 5 μM Fura-2 AM for 30 min and preincubated with inhibitors for 1 h prior to αNF treatment. Fluorescence was monitored throughout each experiment at 37 °C with a fluorescence plate reader (VICTOR luminometer, Perkin-Elmer). After a 5 min temperature equilibration period, the samples were excited at 370 nm, and emission was collected at 476 nm as described (Aires et al., 2007). The concentrations of free intracellular $Ca^{2+}$ were calculated by using the following equation: $[Ca^{2+}]_i = K_d \times (R - R_{min}) / (R_{max} - R)$. A $K_d$ value of 224 nM was used in the calculations. The $R_{max}$ value was obtained by the addition of 5 μM ionomycin and the $R_{min}$ value was obtained by the addition of 2 mM $MnCl_2$, 0.1% Triton X-100, and 2 mM EGTA.

### 2.10. Semiquantitative RT-PCR

Total RNA was extracted from cultured cells using TRI reagent; RT-PCR was performed using an RT-PCR kit according to the manufacturer's instructions. The forward and reverse primer sets for PCR were: 5′−CCGTCCATCCTGGAAATTCGAACC−3′ and 5′−CCTTCTTC ATCGTTAGCGGTCTC−3′ for mouse AhR; 5−GGCCACTTTGACCCTT ACAA−3′ and 5′−CAGGTAACGGAGGACAGGAA−3′ for Cyp1a1; 5′− TCCACCACCCTGTTGCTGTA−3′ and 5′−ACCACAGTCCATGCCATGC CATCAC−3′ for GAPDH. PCR products were visualized on a 1% agarose gel by ethidium bromide staining. GAPDH was used as a loading control.

### 2.11. DRE-luciferase assay

The DRE-Luc plasmid (pGL3-CYP1 A1-luc reporter) was constructed as described previously (Park et al., 2013). The sample wells were washed twice with PBS, followed by the addition of 50 μl cell lysis buffer. Cell lysates were then transferred to 96-well microplates for the measurement of luciferase activity using the Promega dual-luciferase reporter assay system. The firefly luciferase activity was first determined by the addition of 100 μl of Luciferase Assay Reagent II. The resulting luminescence was detected using a luminometer (VICTOR luminometer, Perkin-Elmer). The renilla luciferase activity was subsequently determined following the addition of 100 μL of Stop & Glow Reagent to the same reaction tube. The activity of firefly luciferase was expressed relative to that of renilla luciferase.

### 2.12. Statistical analysis

All data are presented as the mean ± standard deviation of at least three independent experiments. Statistical comparisons were performed using one-way analysis of variance (ANOVA) followed by Tukey's post hoc test for multiple comparisons (Graphpad Prism, Graphpad Software Inc, San Diego, CA, USA). P values of less than 0.05 were considered statistically significant.

## 3. Results

### 3.1. αNF induces apoptotic cell death in HT22 mouse hippocampal neuronal cells

To determine whether αNF induces cell death in HT22 cells, cells were treated with αNF (10–50 μM) for 24 h, and cell viability was examined by MTT assay. The MTT assay showed that αNF reduced cell viability in a dose-dependent manner and the cell viability was reduced to ~45% at 20 μM αNF in HT22 cells (Fig. 1A). To ascertain whether the effect of αNF on cell viability reduction was caused by apoptotic cell death, HT22 cells were treated with 20 μM αNF for 24 h and their DNA contents were examined by flow cytometry. αNF significantly accumulated cells in the sub G1 fraction from 5.8% to 57.1% at 24 h (Fig. 1B), indicating that αNF may induce apoptotic cell death in HT22 cells. Apoptotic cell death was confirmed by an annexin V-FITC/PI double-staining assay. The annexin V-FITC/PI double-staining assay was performed to determine the percentage of early apoptotic (annexin V-positive/PI-negative), late apoptotic (annexin- positive/PI-positive), and necrotic cells (annexin V-negative/PI-positive). Early apoptotic cells were significantly increased from 3.1% to 29.0% at 24 h after treatment with αNF. Under this condition, the fraction of late apoptotic

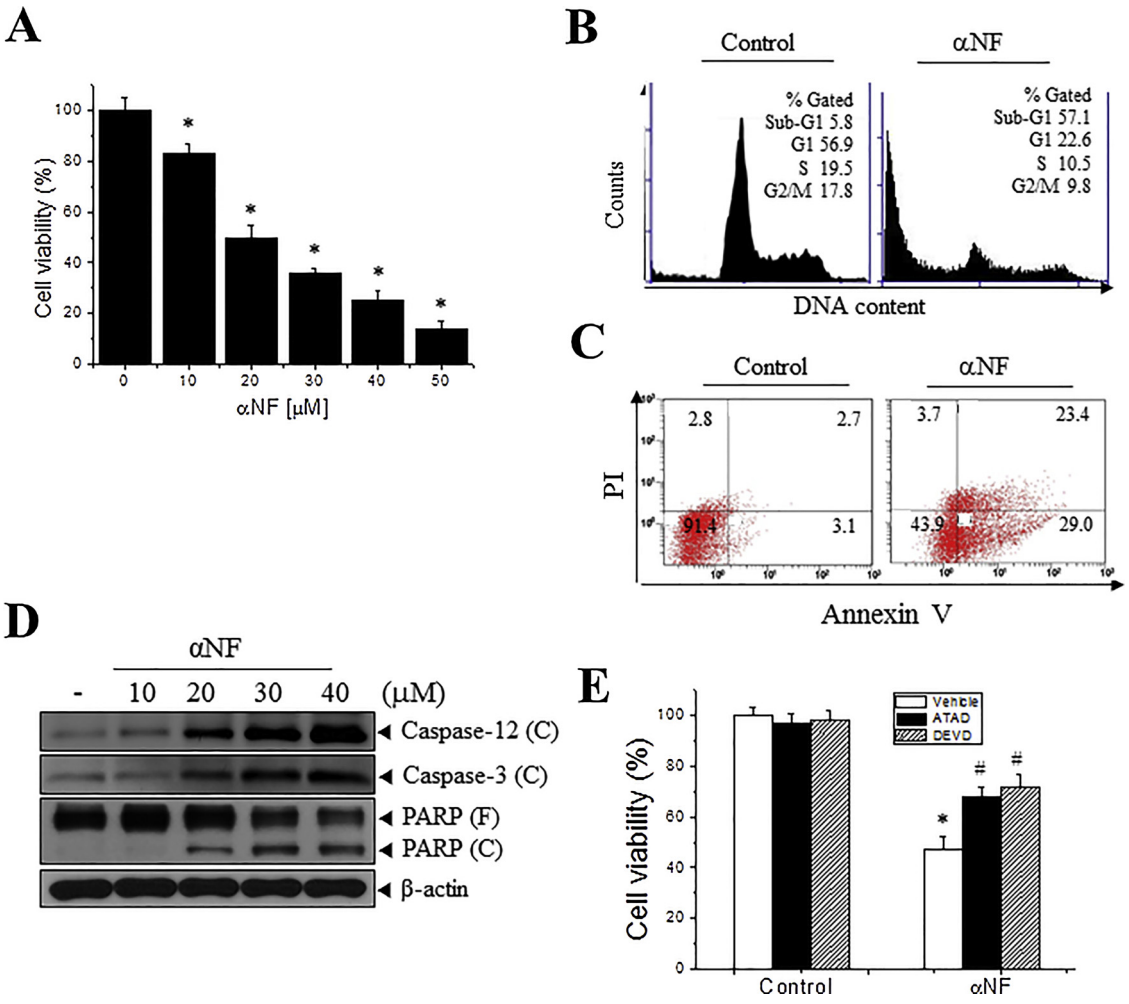


**Fig. 1.** Effects of αNF on cell viability and apoptosis in HT22 mouse hippocampal neuronal cells.
(A) HT22 cells were treated with various concentrations (10 − 50 μM) of αNF for 24 h. Cell viability was determined by MTT assay and the percent viabilities are plotted as the mean ± standard deviation of at least three experiments. $^{*}P < 0.01$ compared with vehicle-treated control cells. (B, C) HT22 cells were treated with vehicle (control) or 20 μM αNF for 24 h. Cell death was evaluated by flow cytometry after staining with PI (B) or annexin V-FITC and PI (C). n = 3 for each experimental group. (D) HT22 cells were treated with 10 − 40 μM αNF for 12 h. The cells were lysed, and total cell extracts were resolved by SDS-PAGE. The protein levels were detected by western blot analysis using antibodies against cleaved form (C) of caspase-12 and caspase-3, the full length PARP(F), cleaved PARP(C), and β-actin. Results shown are representative of more than three independent experiments. (E) HT22 cells were pretreated with an inhibitor of caspase-12 (10 μM Z-ATAD-FMK) or caspase-3 (10 μM Z-DEVD-FMK) for 1 h, and then treated with 20 μM αNF for 24 h. Cell viability was determined by MTT assay and the percent viabilities are plotted as the mean ± standard deviation of at least three experiments. $^{*}P < 0.01$ compared with vehicle-treated control cells. $^{\#}P < 0.01$ compared with αNF alone-treated cells in the presence of vehicle.

cells was increased from 2.7% to 23.4% at 24 h (Fig. 1C). Collectively, these results suggest that αNF induces apoptotic cell death in HT22 cells.

Because caspase activation is one of the mechanisms of apoptotic process, we examined the effect of αNF on caspase activation. HT22 cells were treated with αNF (10–40 μM) for 12 h and activation (cleavage) of caspase-12 and -3 was detected by western blot analysis. Results showed increases in the cleaved fragments of caspase-12 and -3, and PARP by αNF treatment (Fig. 1D). To confirm the role of caspase activation in αNF-induced apoptotic cell death, we used specific inhibitors of caspase-12 (Z-ATAD-FMK) and caspase-3 (Z-DEVD-FMK). HT22 cells were pretreated with 20 μM Z-ATAD-FMK and Z-DEVD-FMK for 1 h and incubated with αNF for 24 h. These caspase inhibitors significantly reversed αNF-induced cell death in HT22 cells (Fig. 1E). The data suggested that caspase activation plays a key role in αNF-induced apoptotic cell death.

### 3.2. αNF induces ER stress-associated proteins in HT22 cells

Because caspase-12 is related to ER stress-induced cell death, we postulated that αNF causes ER stress. To determine whether αNF can increase the expression and activation of ER stress-associated proteins, HT22 cells were treated with αNF or TG as a positive control for ER stress inducer. Using western blot analysis, the effects of αNF on ER stress-associated proteins, such as CHOP expression and eIF2α phosphorylation, were examined. αNF induced CHOP protein expression at 6–24 h (Fig. 2A) and eIF2α phosphorylation at 0.5–2 h (Fig. 2B). However, spliced X-box binding protein (sXBP-1) expression and ATFα cleavage were not observed after αNF treatment (data not shown). The results suggest that the PERK-eIF2α pathway may play an important role in αNF-induced ER stress.

To examine the role of ER stress in αNF-induced apoptotic cell death, a chemical inhibitor of ER stress, salubrinal, was used. HT22 cells were preincubated with 30 μM salubrinal for 1 h and treated with αNF for 24 h. The results showed that salubrinal significantly reduced αNF-or TG-induced cell death in HT22 cells (Fig. 2C), presumably,

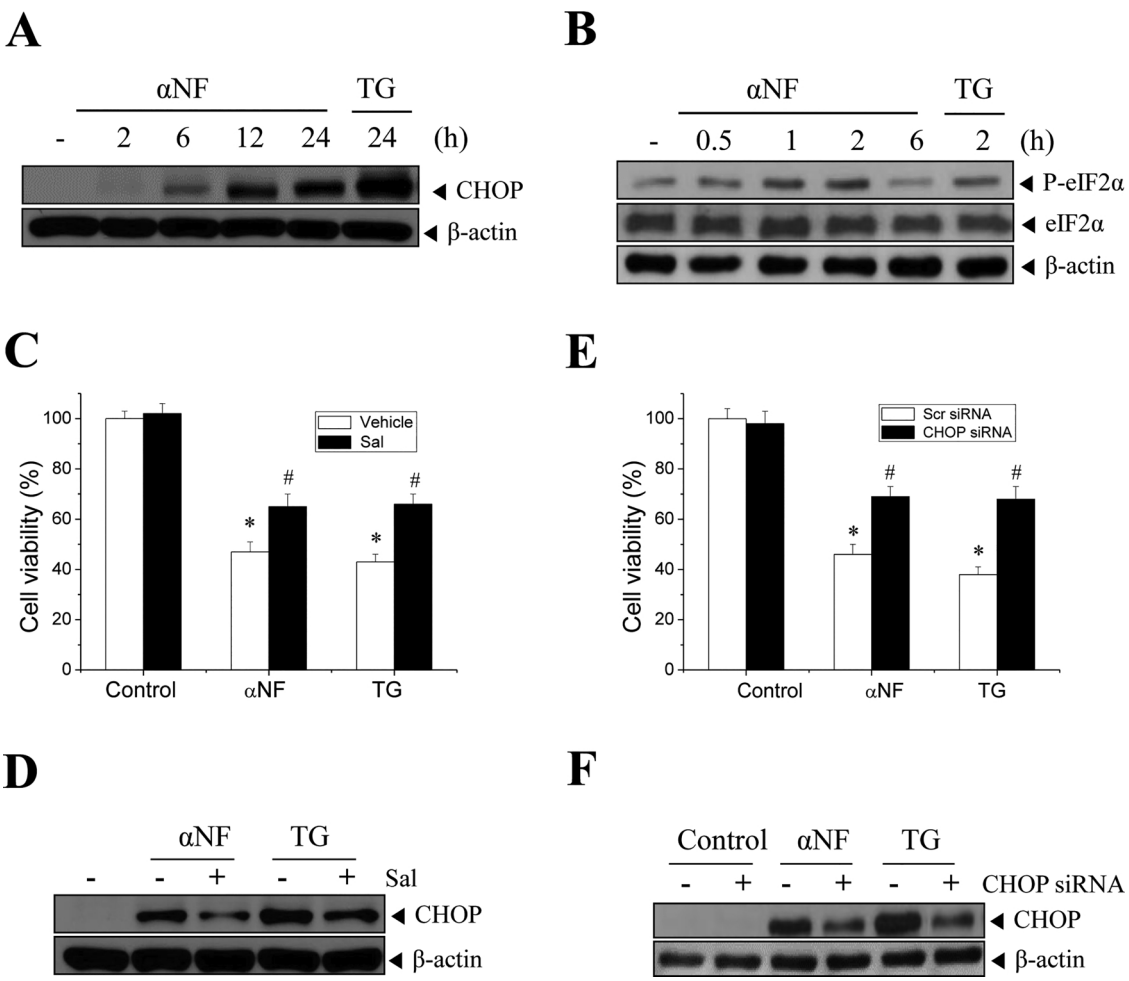


**Fig. 2.** Effects of αNF on the expression of ER stress-associated proteins in HT22 cells.
(A − B) HT22 cells were treated with 20 μM αNF or 1 μM TG for the indicated times. Cell lysates were resolved by SDS-PAGE and analyzed by western blotting with antibodies against CHOP and β-actin (A), and with antibodies against P-eIF2α, eIF2α, and β-actin (B). (C − F) HT22 cells were preincubated with 30 μM salubrinal for 1 h (C and D), or transfected with control scrambled (Scr) or CHOP siRNAs for 24 h (E and F), and then treated with 20 μM αNF for 24 h. Cell viability was determined by MTT assay, and the percent viabilities are plotted as the mean ± standard deviation of at least three experiments (C and E). $^{*}P < 0.01$ compared with vehicle-treated control cells. $^{\#}P < 0.01$ compared with αNF alone- or TG alone-treated cells in the presence of vehicle (Control) or Scr siRNA (E). Cell lysates were separated by SDS-PAGE and analyzed by western blotting with antibodies against CHOP and β-actin (D and F). Results shown are representative of more than three independent experiments.

through reduction of CHOP (Fig. 2D). To confirm the role of ER stress and CHOP induction in αNF-induced apoptotic cell death, CHOP expression was inhibited by transfection with CHOP siRNA for 24 h, the effects of αNF on cell viability were then examined at 24 h. Knockdown of CHOP partially blocked αNF- and TG-induced cell death in HT22 cells (Fig. 2E and F). Collectively, these data suggest that ER stress and CHOP expression contribute to αNF-induced cell death in HT22 cells.

### 3.3. MAPKs play a role in αNF-induced cell death and CHOP expression in HT22 cells

Previous studies have demonstrated that activation of MAPKs, such as p38, JNK, and ERK, is involved in ER stress- and mitochondrial dysfunction-induced apoptosis (Choi et al., 2011, 2017). Therefore, we attempted to determine whether αNF regulates MAPK activation using western blot analysis. As shown in Fig. 3A, αNF increased the phosphorylation (activation) of p38, JNK, and ERK. To understand the functional role of MAPKs in αNF-induced apoptosis, cells were pretreated with specific inhibitors of p38 (10 μM SB203580), JNK (10 μM SP600125), and ERK-upstream molecule MAPK/ERK kinase (MEK) (20 μM PD98059), followed by treatment with αNF for 24 h. The results showed that treatment of HT22 cells with these inhibitors significantly blocked αNF-induced cell death (Fig. 3B). Treatment with the inhibitors resulted in a reduction of αNF-induced CHOP expression (Fig. 3C). The data suggest that αNF induces cell death and CHOP expression through activation of MAPKs. To confirm the role of MAPKs activation in αNF-induced apoptosis, cells were transfected with siRNAs for MAPKs for 24 h, followed by treatment with αNF for 24 h. The results showed that knockdown of MAPKs reversed αNF-induced cell death as well as CHOP expression (Fig. 3D and E). These data suggest that MAPK activation might be responsible for αNF-induced ER stress and subsequent apoptotic cell death in HT22 cells.

### 3.4. αNF induces cell death through ROS accumulation and mitochondrial dysfunction in HT22 cells

Accumulation of ROS is a key event of the apoptotic pathway and involvement of ROS in ER stress-induced apoptosis has been demonstrated (Choi et al., 2010). Therefore, we attempted to determine whether αNF induces accumulation of ROS in HT22 cells. Cells were treated with αNF for 1–6 h and cellular ROS levels were measured using flow cytometry after treatment with DCFH-DA for 30 min. The result showed that αNF induced ROS accumulation (Fig. 4A).

To understand the role of ROS in cell death, we examined the effect

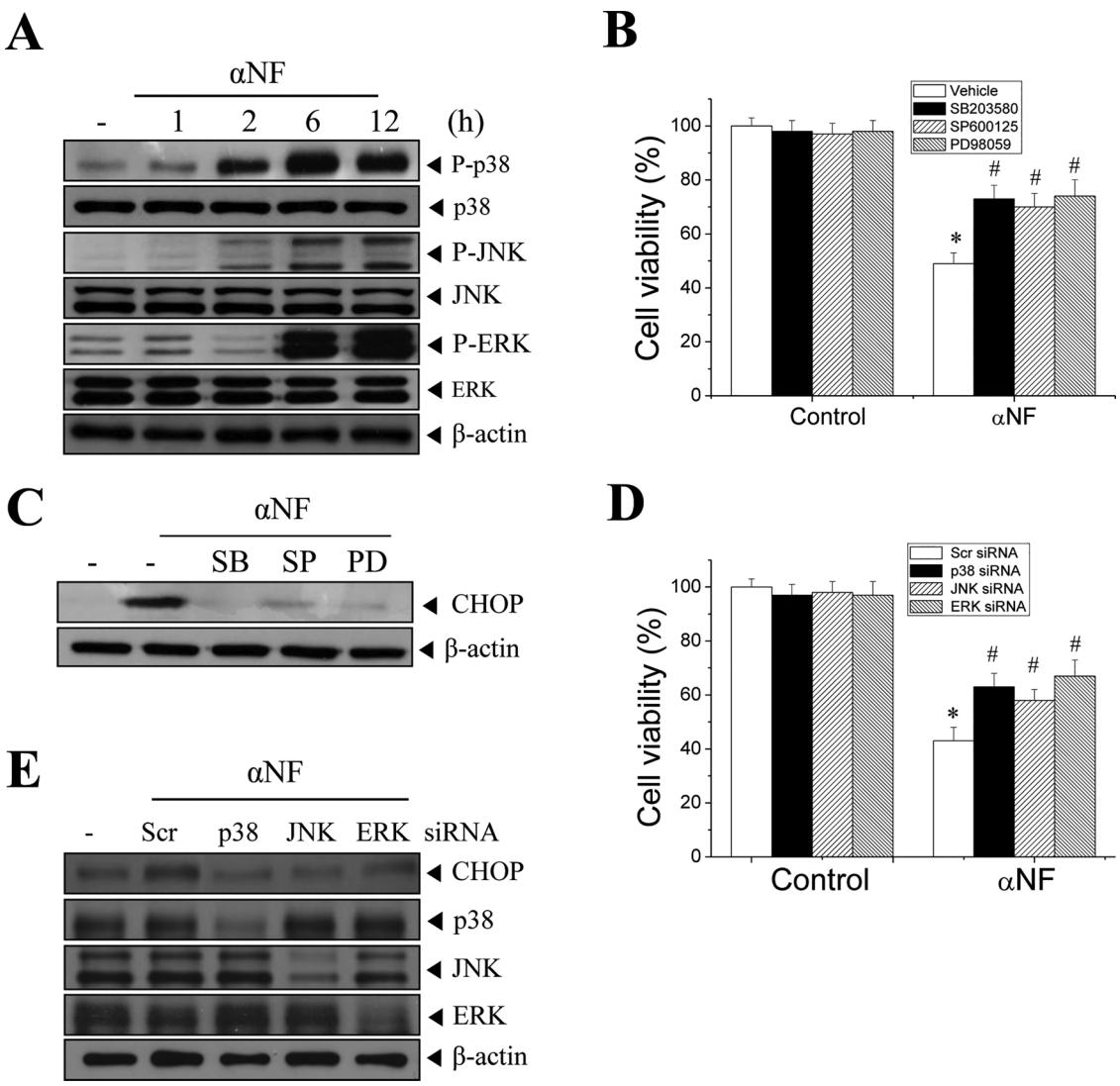


**Fig. 3.** Effects of αNF on the activation of MAPK family in HT22 cells.
(A) HT22 cells were treated with 20 μM αNF for the indicated times (1 − 12 h). Cell lysates were resolved by SDS-PAGE and analyzed by western blotting with antibodies specific to phospho-p38 (P-p38), p38, phospho-JNK (P-JNK), JNK, phospho-ERK (P-ERK), ERK, and β-actin. (B − E) HT22 cells were preincubated with the MAPK inhibitors (10 μM SB203580, 10 μM SP600125, 20 μM PD98059) for 1 h (B and C) or transfected with scrambled (Scr) control, p38α, JNK, or ERK siRNAs for 24 h (D and E), and then treated with αNF for 24 h. Cell viability was determined by MTT assay and the percent viabilities are plotted as the mean ± standard deviation of at least three experiments. *P < 0.01 compared with vehicle-treated (B) or Scr siRNA-treated cells (D). #P < 0.01 compared with αNF alone-treated cells in the presence of vehicle (B) or Scr siRNA (D). Cell lysates were analyzed by western blotting with antibodies against CHOP, p38, JNK, ERK, and β-actin. Results shown are representative of more than three independent experiments.

of a well-known antioxidant, NAC, on αNF-induced apoptosis and ER stress. Cells were preincubated with 5 mM NAC for 1 h and followed by αNF treatment for 24 h, and then cell death was examined. The results showed that NAC inhibited apoptotic cell death (Fig. 4B) and blocked the CHOP expression in αNF-treated HT22 cells (Fig. 4C). We then determined whether αNF-induced MAPK activation is associated with ROS production. Cells were preincubated with NAC for 1 h and followed by αNF treatment and MAPKs phosphorylation was examined. The results showed that NAC reduced αNF-induced MAPK activation (Fig. 4D). These data suggest that ROS act as upstream signaling for αNF-induced MAPK activation in HT22 cells.

ROS could induce mitochondrial dysfunction-induced apoptotic death (Choi et al., 2010). Therefore, to understand whether mitochondrial dysfunction is involved in αNF-induced apoptosis, we examined the effect of αNF on mitochondrial membrane potential (MMP) loss in HT22 cells. For the measurement of MMP loss, cells were treated with αNF for 12 h. After incubation with $DiOC_6$ for 30 min, MMP was measured using flow cytometry. The data showed that the levels of MMP decreased to ~ 60% at 12 h after treatment with αNF (Fig. 4E). We next examined the role of ROS in αNF-induced MMP loss. Cells were preincubated with NAC for 1 h and followed by αNF treatment, and then MMP loss was examined. The results showed that NAC reduced αNF-induced MMP loss (Fig. 4F). These data suggest an important role for ROS in αNF-induced apoptotic cell death by acting upstream of mitochondrial dysfunction in HT22 cells.

### 3.5. αNF induces cell death through $Ca^{2+}$ influx in HT22 cells

Cytosolic $Ca^{2+}$ plays an important role in the regulation of cell death and survival (Choi et al., 2011; Gordeeva et al., 2003). It has been shown that the exposure to AhR ligands, such as αNF, dioxin, and benzo[*a*]pyrene, increases intracellular $Ca^{2+}$ levels as well as extracellular $Ca^{2+}$ fluxes (Cheng et al., 2003; Morales-Hernandez et al., 2012). Therefore, we examined whether $Ca^{2+}$ plays a role in αNF-induced cell death and ER stress. We measured the level of cytosolic $Ca^{2+}$ with a fluorescent plate reader after cells were stained with $Ca^{2+}$-sensitive

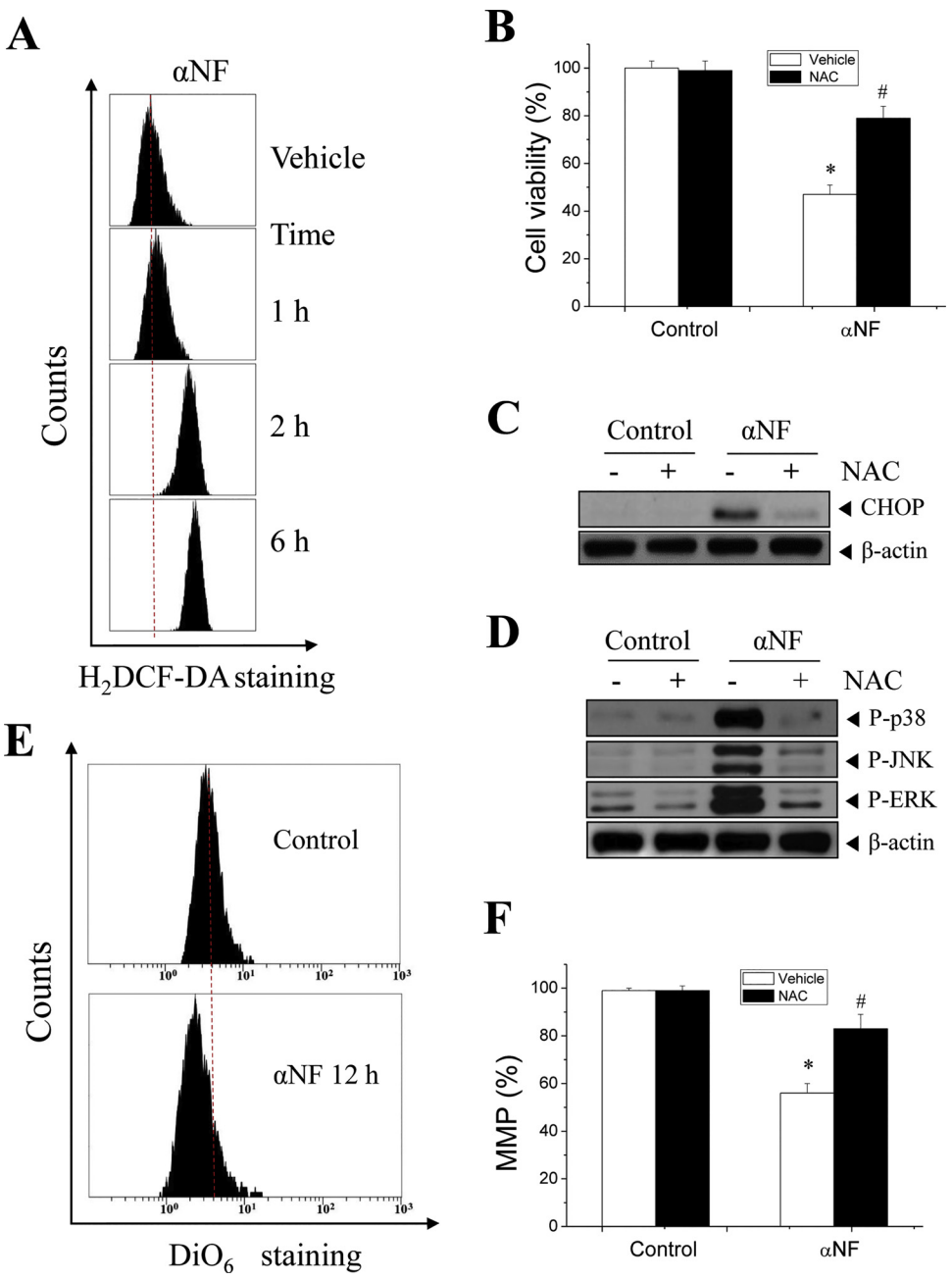


**Fig. 4.** Effects of αNF on ROS generation and MMP loss in HT22 cells.
(A) HT22 cells were incubated with 20 μM αNF for the indicated times. Cells were then treated with 10 μM DCF-DA for 30 min and DCF fluorescence as an indication of the amount of ROS was measured by flow cytometry. (B) HT22 cells were preincubated with 5 mM NAC for 1 h and then treated with αNF for 24 h. Cell viability was determined by MTT assay and the percent viabilities are plotted as the mean ± standard deviation of at least three experiments. (C, D) HT22 cells were preincubated with 5 mM NAC for 1 h and treated with αNF for 24 h (C) or 6 h (D). Cell lysates were separated by SDS-PAGE and analyzed by western blotting with antibodies specific to CHOP, P-p38, P-JNK, P-ERK, and β-actin. Results shown are representative of more than three independent experiments. (E, F) Cells were incubated with 20 μM αNF for 12 h (E) or preincubated with 5 mM NAC for 1 h and followed by αNF for 12 h (F). After each treatment, cells were incubated with 20 nM $DiOC_6$ for 30 min and MMP was measured using flow cytometry. The percent MMP was calculated and plotted as the mean ± standard deviation of at least three experiments. In (B) and (F), *P < 0.01 compared with vehicle-treated control cells. #P < 0.01 compared with αNF alone-treated cells in the presence of vehicle.

fluorescent dye, Fura-2 AM, for 30 min. We found that αNF markedly induced cytosolic $Ca^{2+}$ elevation and showed substantial reduction of fluorescent signals in the absence of $Ca^{2+}$ in the extracellular medium (Fig. 5A), suggesting that αNF induces extracellular $Ca^{2+}$ influx. To verify that cytosolic $Ca^{2+}$ accumulation is involved in αNF-induced ER stress and apoptotic cell death, cells were pretreated with EGTA (0.5 and 1 mM), a chelator of extracellular $Ca^{2+}$, and followed by αNF for 24 h. Pretreatment with EGTA reduced αNF-induced cell death and CHOP expression (Fig. 5B and C). The role of extracellular $Ca^{2+}$ influx was also examined in αNF-induced MMP loss. Cells were preincubated with 1 mM EGTA for 1 h and followed by αNF treatment, and then MMP loss was examined. The results showed that EGTA reduced αNF-induced MMP loss (Fig. 5D). These data suggest an important role of $Ca^{2+}$ influx in αNF-induced apoptotic cell death by acting upstream of mitochondrial dysfunction in HT22 cells.

### *3.6. c-Src plays a role in αNF-induced cell death and CHOP induction via ROS accumulation in HT22 cells*

Previously, it has been reported that c-Src tyrosine kinase is activated by dioxin and mediates AhR signaling through a nongenomic pathway (Matsumura, 2009; Tomkiewicz et al., 2013; Xie et al., 2012). Therefore, we attempted to determine whether αNF regulates c-Src activation using western blot analysis. As shown in Fig. 6A, αNF induced an increase in phosphorylation (activation) of c-Src at Tyr416. In order to understand the functional role of c-Src in αNF-induced apoptosis and ER stress, cells were pretreated with the specific inhibitor of c-Src (10 and 20 μM SU6656) followed by treatment with αNF for 24 h. The results showed that treatment of HT22 cells with SU6656 significantly blocked αNF-induced cell death and CHOP expression (Fig. 6B and C). These data suggest that αNF induces cell death and CHOP expression through activation of c-Src. To confirm the roles of c-Src in αNF-induced cell death and ER stress, cells were transfected with c-Src siRNA for 24 h and followed by treatment with αNF. The results

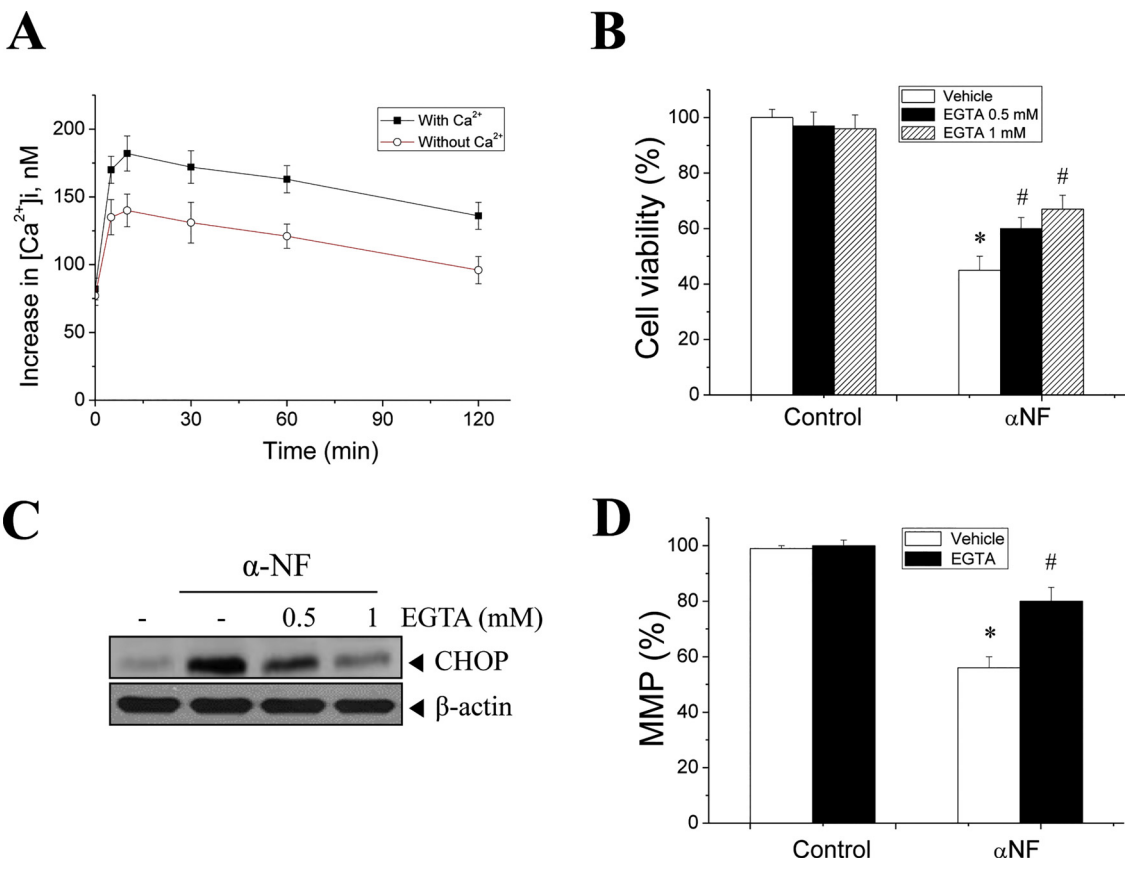


**Fig. 5.** Effects of $Ca^{2+}$ on αNF-induced cell death and MMP loss in HT22 cells.
(A) HT22 cells were incubated with 20 μM αNF for the indicated times with or without extracellular $Ca^{2+}$ and then loaded with Fura-2 AM for 30 min. Fluorescence was monitored at 37 °C with a fluorescent plate reader. Intracellular $Ca^{2+}$ changes (Δ increase in $[Ca^{2+}]i$) were calculated and plotted. (B) Cells were incubated in the presence of EGTA (0.5, 1 mM) for 1 h and followed by 20 μM αNF for 24 h. Cells were assessed for the cell viability by MTT assay and the percent viabilities are plotted as the mean ± standard deviation of at least three experiments. (C) HT22 cells were preincubated with 0.5 and 1 mM EGTA for 1 h and followed by αNF treatment for 24 h. Cell lysates were analyzed by western blotting with antibodies specific to CHOP and β-actin. Results shown are representative of more than three independent experiments. (D) Cells were preincubated with vehicle or EGTA for 1 h and followed by αNF treatment for 12 h. After each treatment, cells were incubated with 20 nM $DiOC_6$ for 30 min and MMP was measured using flow cytometry. The percent MMP was calculated and plotted as the mean ± standard deviation of at least three experiments. In (B) and (D), *P < 0.01 compared with vehicle-treated control cells. #P < 0.01 compared with αNF alone-treated cells in the presence of vehicle.

showed that knockdown of c-Src reversed αNF-induced cell death as well as CHOP expression (Fig. 6D and E). These data suggest that c-Src activation is responsible for αNF-induced ER stress and apoptotic cell death in HT22 cells.

In addition, we determined whether αNF-induced activation of c-Src is associated with ROS production. Cells were preincubated with SU6656 for 1 h and followed by αNF treatment and ROS accumulation was examined. The results showed that SU6656 reduced ROS accumulation (Fig. 6F). These data suggest that c-Src is an upstream signaling for αNF-induced ROS accumulation in HT22 cells. Furthermore, we determined whether αNF-induced activation of MAPKs is associated with c-Src activation. Cells were preincubated with SU6656 for 1 h and followed by αNF treatment, and then MAPK phosphorylation was examined. The results showed that SU6656 reduced MAPK phosphorylation (Fig. 6G). These data suggest that c-Src acts as an upstream signaling for αNF-induced MAPK activation in HT22 cells.

### *3.7. αNF induces apoptotic cell death in an AhR- and ARNT-dependent manner in HT22 cells*

Because AhR-dependent and independent effects are reported for various AhR ligands, we first examined the effect of αNF on the expressions of AhR and its target gene, Cyp1a1. Cells were treated with αNF and analyzed the protein and mRNA expressions of AhR and Cyp1a1 by western blot analysis and RT-PCR, respectively. The result showed that αNF did not significantly affect the protein and mRNA expressions of AhR itself, while it increased those of Cyp1a1 (Fig. 7A). To examine whether AhR mediates αNF-induced cell death and ER stress in HT22 neuronal cells, a well-known AhR antagonist, CH223191, was used. Cells were pretreated with 10 μM CH223191 and treated with αNF or TG for 24 h, and then cell viability as well as CHOP expression was measured. The result showed that CH223191 significantly blocked αNF-induced cell death and CHOP expression (Fig. 7B and C). As expected, CH223191 had no effects on TG-induced cell death and CHOP expression. To confirm the involvement of AhR in αNF-induced cell death and CHOP expression, cells were transfected with AhR siRNA and treated with αNF for 24 h. The results showed that knockdown of AhR reduced αNF-induced cell death and CHOP expression (Fig. 7D and E). We also examined the loss of function of AhR in AhR siRNA experiments using αNF and a prototypical AhR agonist TCDD. As expected, AhR knockdown significantly reduced the expression of Cyp1a1 mRNA in αNF- and TCDD- treated HT22 cells (Fig. 7F). These data suggest that AhR mediates αNF-induced cell death and ER stress in HT22 cells. In the present experiment, we also examined the involvement of ARNT in αNF-induced cell death and ER stress. Cells were transfected with ARNT siRNA and treated with αNF for 24 h. The results showed that knockdown of ARNT also reduced αNF-induced cell death and CHOP expression (Fig. 7G and H). Cells were transfected with

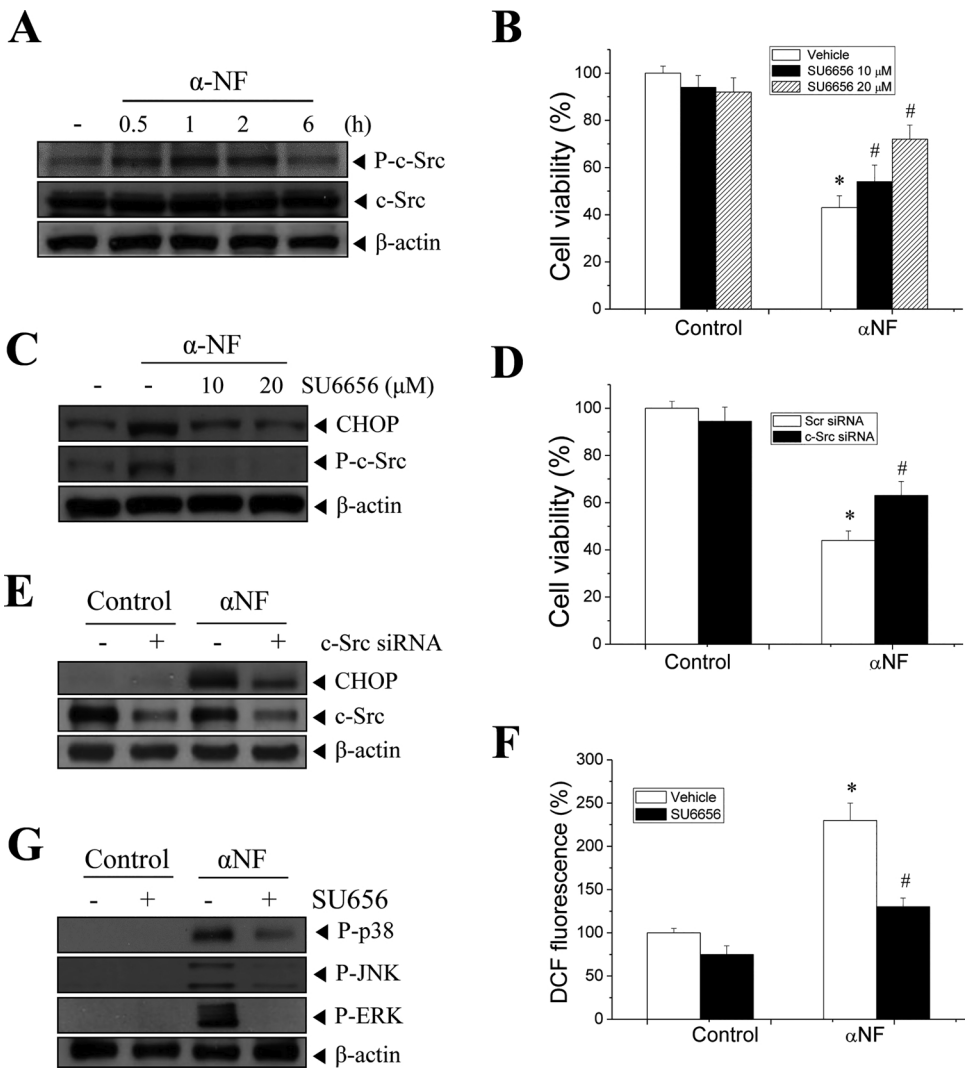


**Fig. 6.** Effects of αNF on the activation of c-Src in HT22 cells.
(A) HT22 cells were treated with 20 μM αNF for the indicated times. Cell lysates were resolved by SDS-PAGE and analyzed by western blotting with antibodies specific to phospho-c-Src (P-c-Src), c-Src, and β-actin. (B – E) HT22 cells were preincubated with a c-Src inhibitor (10 or 20 μM SU6656) for 1 h (B and C) or pretreated with scrambled (Scr) control or c-Src siRNA for 24 h (D and E), and then treated with αNF for 24 h. Cell viability was determined by MTT assay and the percent viabilities are plotted as the mean ± standard deviation of at least three experiments. Cell lysates were analyzed by western blotting with antibodies specific to CHOP, P-c-Src, c-Src, and β-actin. Results shown are representative of more than three independent experiments. (F, G) HT22 cells were preincubated with 20 μM SU6656 for 1 h and αNF for 12 h (F) or 6 h (G). Cells were then treated with 10 μM DCF-DA for 30 min and DCF fluorescence was measured by flow cytometry. Percent ROS generation is calculated from DCF fluorescence and plotted as the mean ± standard deviation of at least three experiments. Cell lysates were analyzed by western blotting with antibodies specific to P-p38, P-JNK, P-ERK, and β-actin (G). In (B), (D), and (F), *P < 0.01 compared with vehicle-treated or Scr siRNA-treated control cells. #P < 0.01 compared with αNF alone-treated cells in the presence of vehicle or Scr siRNA.

ARNT siRNA and treated with αNF for 24 h. The results showed that knockdown of ARNT also reduced αNF-induced cell death and CHOP expression (Fig. 7G and H). Collectively, these data suggest that AhR/ARNT-dependent genomic pathway may play a role in αNF-induced cell death and ER stress in HT22 cells.

### *3.8. αNF acts as an AhR agonist that induces transcriptional activation of AhR in HT22 neuronal cells*

αNF is known as an antagonist but it also has a partial agonistic activity for AhR (Murray et al., 2011; Santostefano et al., 1993). Since the agonistic and antagonistic activities of AhR ligands may differ depending on cells, species, and other contexts, we examined the effect of αNF on AhR-responsivetranscriptional activity in HT22 cells using a plasmid with DRE-luciferase reporter gene (pDRE-Luc). After transfection with the pDRE-Luc plasmid, cells were pretreated with CH223191 or transfected with AhR or ARNT siRNA, and followed by αNF for 24 h. Cells were then examined DRE transcriptional activity. The results showed that αNF induced DRE-luciferase activity and it was blocked by CH223191 and AhR or ARNT siRNA transfection in HT22 cells (Fig. 8A). The results suggest that αNF acts as an AhR agonist and induces transcriptional activation of AhR in HT22 moue hippocampal neuronal cells.

In this study, MAPKs are mediators of αNF-induced ER stress and cell death (Fig. 3), thus, we examined whether these upstream signaling molecules participate in αNF-induced transcriptional activation of AhR. After transfection with the pGL3-DRE-Luc plasmid, cells were pretreated with MAPK inhibitors or MAPK siRNAs and followed by αNF for 24 h. The results showed that inhibition of MAPKs reduced αNF-induced DRE-luciferase activity (Fig. 8B and C). These results suggest that MAPKs mediate αNF-induced transcriptional activation of AhR in HT22 cells. Since c-Src mediates αNF-induced ER stress and cell death (Fig. 6), the role of c-Src in transcriptional activation of AhR was also examined using the pGL3-DRE-Luc plasmid-transfected cells that were pretreated with SU6656 or c-Src siRNA and followed by αNF for 24 h. The results showed that c-Src inhibition reduced αNF-induced DRE-luciferase activity (Fig. 8D). Consistent with its effect on DRE-luciferase activities, c-Src inhibition by SU6656 or c-Src siRNA transfection reduced αNF-induced Cyp1a1 mRNA (Fig. 8E and F). Collectively, these results suggest that c-Src mediate αNF-induced transcriptional activation of AhR and thus cell death though genomic pathway in HT22 cells.

## 4. Discussion

Environmental pollutants have toxic effects to many organs, including the liver, skin, and nervous system (Bock, 2016; Chepelev et al., 2015; Chopra and Schrenk, 2011; Williamson et al., 2005). For example, environmental exposure to benzo[*a*]pyrene was shown to be correlated with impaired learning and memory, and poor neurodevelopment in human (Chepelev et al., 2015). The prototypical dioxin, TCDD, was also reported to induce cognitive disability and motor dysfunction during development and adulthood (Kakeyama and

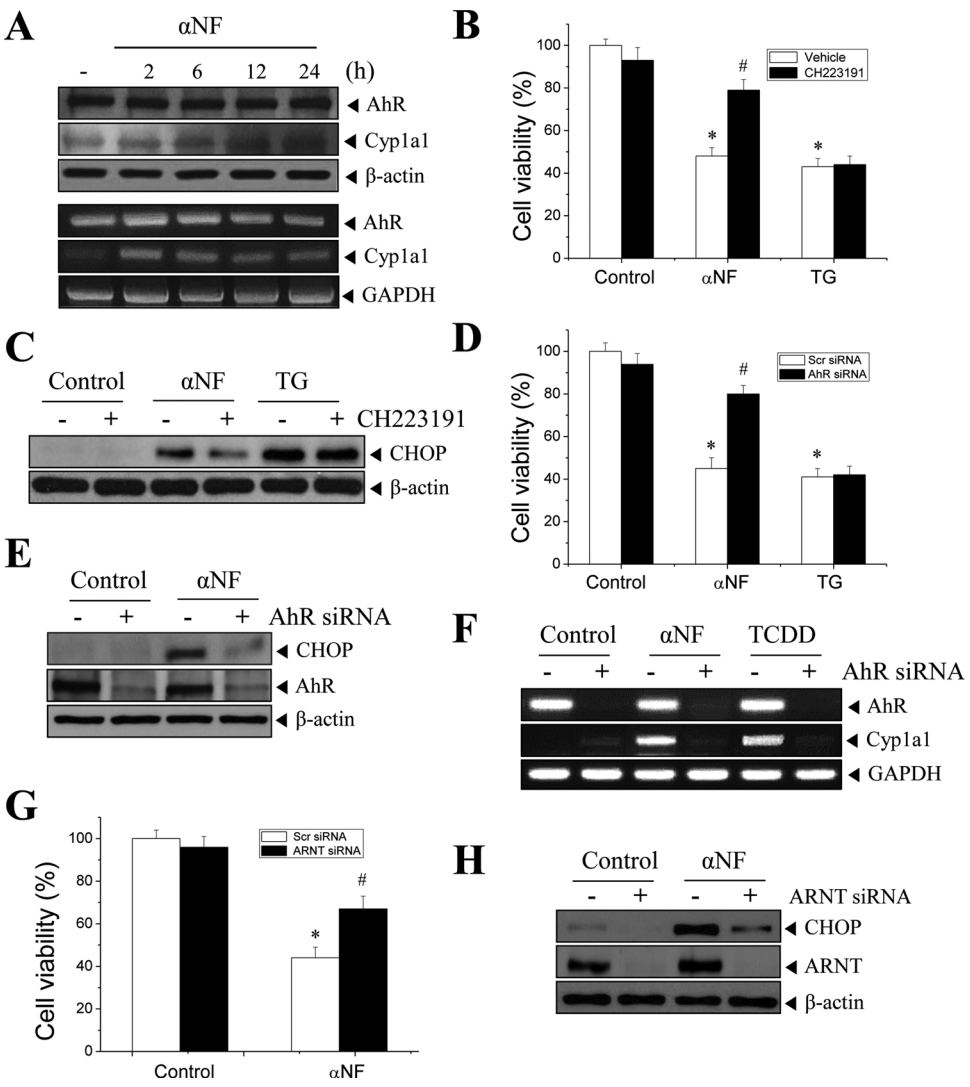


**Fig. 7.** Roles of AhR and ARNT in αNF-induced cell death and CHOP expression in HT22 cells. (A) HT22 cells were treated with 20 μM αNF for the indicated times. Cell lysates were resolved by SDS-PAGE and analyzed by western blotting with antibodies specific to AhR, Cyp1a1, and β-actin (upper panels). Samples containing 1 μg total RNA were subjected to RT–PCR to determine AhR, Cyp1a1, and GAPDH mRNA levels (lower panels). (B, C) HT22 cells were preincubated with 20 μM CH223191 for 1 h and then treated with αNF or TG for 24 h. Cell viability was determined by MTT assay and the percent viabilities are plotted as the mean ± standard deviation of at least three experiments (B). Cell lysates were then analyzed by western blotting with antibodies specific to CHOP and β-actin (C). (D–H) HT22 cells were transfected with control scrambled (Scr), AhR, or ARNT siRNAs for 24 h, and then treated with αNF or TG for 24 h (for cell viability or western blotting) or αNF or 30 nM TCDD for 6 h (for RT-PCR). Cell viability was then determined by MTT assay and the percent viabilities are plotted as the mean ± standard deviation of at least three experiments (D and G). Cell lysates were resolved by SDS-PAGE and analyzed by western blotting with antibodies specific to CHOP, AhR, ARNT, and β-actin (E and H). Samples containing 1 μg total RNA were subjected to RT–PCR to determine AhR, Cyp1a1, and GAPDH mRNA levels (F). Results shown are representative of more than three independent experiments. In (B), (D), and (G), *P < 0.01 compared with vehicle-treated or Scr siRNA-treated control cells. #P < 0.01 compared with αNF alone-treated cells in the presence of vehicle or Scr siRNA.

Tohyama, 2003; Nishijo et al., 2007). Because these pollutants exert their effects through AhR activation and modulation, they are called as AhR ligands (Denison and Nagy, 2003; Song and Pollenz, 2002). Previous reports have shown that AhR ligands exert their effects through the AhR-dependent and/or –independent manner (Butler et al., 2004; Jeon et al., 2002; Lee et al., 2011; Sanchez-Martin et al., 2011; Yoshioka et al., 2012). AhR ligands can also exert the agonistic and/or antagonistic activities, and both anti- and pro-apoptotic functions, depending on cell types, species, and other cellular contexts (Kajta et al., 2009; Lin et al., 2009; Murray et al., 2011; Zhu et al., 2017). According to these previous reports, it is suggested that the more complicated mechanisms might be involved in the AhR ligand-induced signaling pathways. For example, despite several studies on the toxic effects of TCDD in neuronal cells (Morales-Hernandez et al., 2016, 2012; Sanchez-Martin et al., 2011), the molecular mechanisms of AhR ligand-induced neurotoxicity remain to be elucidated.

ER stress-mediated apoptosis is a key pathologic event in the neurological disease processes and neuronal cell death (Lindholm et al., 2006). Therefore, we examined whether ER stress is involved in apoptosis induced by αNF in HT22 mouse hippocampal neuronal cells. In the present study, we found that αNF induces apoptosis of HT22 cells, as proven by annexin V and PI double-staining (Fig. 1C). Moreover, caspase-12, localized in the ER membrane, was shown to be one of pro-apoptotic factors in αNF-treated HT22 cells (Fig. 1D). In agreement with the effect of αNF on caspase-12 activation, αNF induced changes in other ER stress-associated proteins, such as eIF2α and CHOP (Fig. 2A and B). The role of CHOP expression and ER stress in αNF-induced apoptosis was confirmed by treatment with an ER stress inhibitor, salubrinal, or knockdown of CHOP by siRNA transfection (Fig. 2C-F). Interestingly, in this study, unlike eIF2α phosphorylation, sXBP-1 expression and ATFα cleavage were not induced by αNF treatment (data not shown), suggesting that the PERK-eIF2α pathway, but not IRE1 and ATF6 pathways, may play a significant role in αNF-induced ER stress. In agreement with our observations, two other AhR ligands, TCDD and FICZ (6-formylindole (3, 2-b) carbazole), induced activation of PERK-eIF2α pathway, but not IRE1 and ATF pathways, in PC12 cells and mast cells, respectively (Duan et al., 2014; Wang et al., 2017).

Next, we examined how αNF induces ER stress and cell death in HT22 cells. Previously, activation of MAPKs (p38, JNK, and ERK), accumulation of intracellular ROS, and mitochondrial dysfunction have been located upstream of the ER stress pathway (Choi et al., 2010). Furthermore, the AhR signaling pathway has included activation of MAPKs (Henklova et al., 2008; Puga et al., 2009), and ROS production (Wang et al., 2017). Therefore, we investigated the effect of αNF on the MAPK activity and intracellular ROS level in HT22 cells. In this study, we found that αNF increased phosphorylation and activation of MAPKs (Fig. 3A). MAPK activation may be necessary for CHOP expression and apoptotic cell death, as judged by the reversing effect of MAPK inhibitors, SB203580, SP600125, and PD98059, and MAPK siRNAs (Fig. 3B-E). αNF also induced ROS production (Fig. 4A) and MMP loss

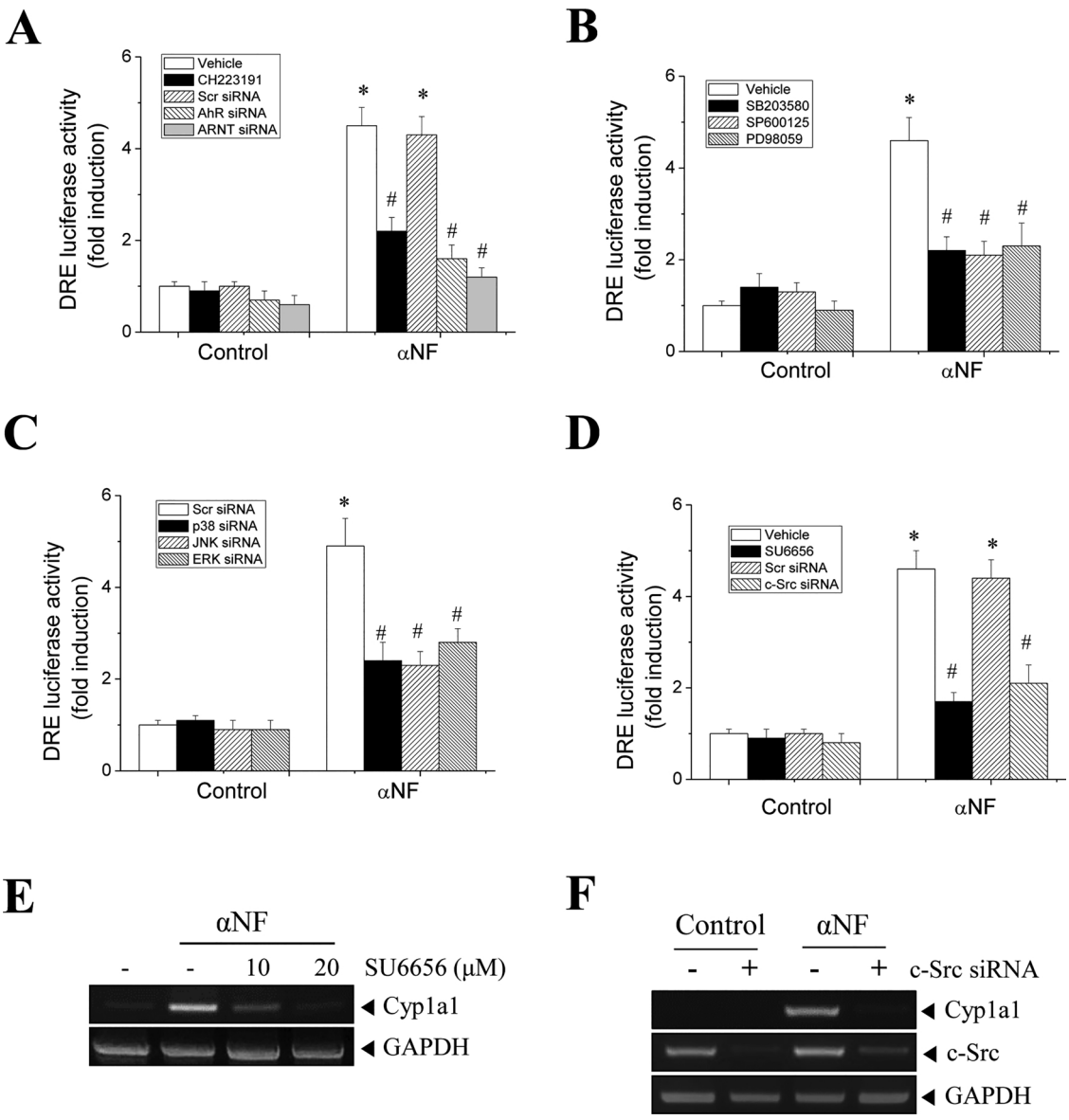


**Fig. 8.** Effect of αNF on the AhR-responsive DRE luciferase activity and Cyp1a1 mRNA expression in HT22 cells.
(A) HT22 cells were transfected with a plasmid containing AhR-responsive element DRE and luciferase reporter gene (pDRE-Luc) for 24 h and were preincubated with 20 μM CH223191 for 1 h or transfected with Scr and AhR siRNAs for 24 h and then treated with 20 μM αNF for 24 h. (B, C) HT22 cells were transfected with pDRE-Luc for 24 h and were preincubated with SB203580, SP600125, and PD98059 for 1 h (B) or transfected with Scr and MAPKs (p38, JNK, ERK) siRNAs for 24 h (C), and then treated with αNF for 24 h. (D) HT22 cells were transfected with pDRE-Luc for 24 h and were preincubated with SU6656 for 1 h or transfected with Scr and c-Src siRNAs for 24 h and then treated with αNF for 24 h. The AhR-responsive DRE luciferase activities were measured by a luminometer. Data are expressed as the mean relative DRE luciferase activities (fold induction) ± standard deviation of at least three experiments (A–D). $^{*}P < 0.01$ compared with vehicle- or Scr siRNA-treated control cells. $^{\#}P < 0.01$ compared with αNF alone-treated cells in the presence of vehicle or Scr siRNA. (E, F) HT22 cells were pretreated with SU6656 for 1 h (E) or transfected with c-Src siRNA for 24 h (F), and then treated with αNF for 6 h. Samples containing 1 μg total RNA were subjected to RT–PCR to determine mRNA levels of Cyp1a1, c-Src, and GAPDH. Results shown are representative of more than three independent experiments.

(Fig. 4E). Since the antioxidant, NAC, reduced αNF-induced MMP loss, MAPKs phosphorylation, CHOP expression, and cell death (Fig. 4B-D), it is suggested that ROS production might be an upstream event of mitochondrial dysfunction and MAPKs, which initiate ER stress-induced apoptotic process in αNF-treated HT22 cells.

Previously, accumulation of intracellular $Ca^{2+}$ has also been located upstream of the ER stress pathway (Choi et al., 2010). Furthermore, the exposure of cells to the AhR ligand increases intracellular $Ca^{2+}$ concentration from intracellular store or extracellular influx in other systems (Cheng et al., 2003; Morales-Hernandez et al., 2012). Therefore, we investigated the effect of αNF on the intracellular $Ca^{2+}$ level in HT22 cells. In the present study, we found that αNF induced cytosolic $Ca^{2+}$ accumulation (Fig. 5A). Because chelation of extracellular $Ca^{2+}$ with EGTA blocked αNF-induced MMP loss, CHOP expression, and cell death (Fig. 5B-D), extracellular $Ca^{2+}$ influx may play a role upstream of mitochondrial dysfunction, which might be responsible for ER stress and cell death in the cells. In agreement with our study, αNF has also been shown to induce vasodilation through induction of extracellular $Ca^{2+}$ influx in endothelium (Cheng et al., 2003). Interestingly, TCDD is shown to induce $Ca^{2+}$ entry and knockdown of the AhR attenuates NMDA-induced excitotoxicity and intracellular $Ca^{2+}$ elevation in cortical neurons (Lin et al., 2009, 2008). Although the NMDA receptor is well-known to be a ligand-gated $Ca^{2+}$ channel that plays a key role in glutamate-induced excitotoxicity (Rao and Finkbeiner, 2007), the relationship between AhR and NMDA receptor in HT22 cells is not clarified. Previously, it was reported that differentiation of HT22 cells

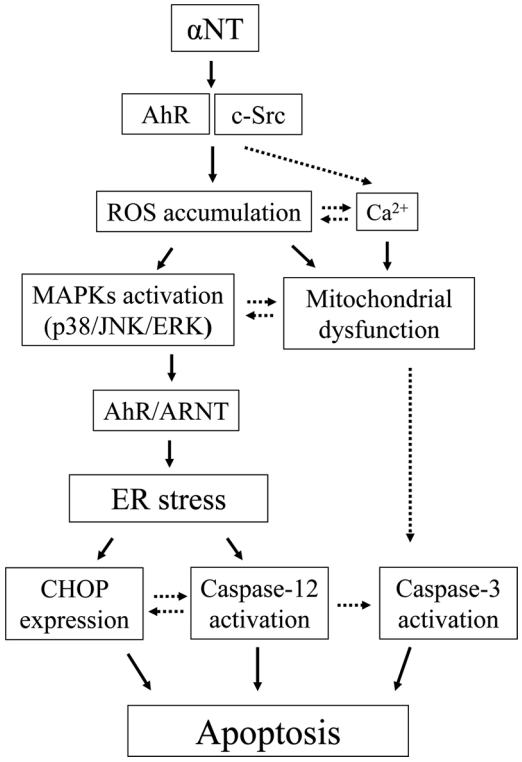


**Fig. 9.** Schematic representation of the proposed model of the αNF-induced apoptosis pathway in HT22 neuronal precursor cells. αNF induces AhR and c-Src activation, cytosolic ROS and $Ca^{2+}$ accumulation, MAPKs activation, and mitochondrial dysfunction. Subsequently, αNF induces ER stress and CHOP expression in an AhR/ARNT-dependent manner. When the interactions between the items are proven, they are indicated by solid arrows. If the interactions are predicted by other articles, they are indicated by dashed arrows. Both ER stress and mitochondrial dysfunction might be responsible for αNF-induced apoptotic cell death in HT22 cells.

significantly increases the NMDA receptor expression (Zhao et al., 2012). In agreement with the expression levels, the differentiated HT22 cells become much more sensitive to glutamate and homocysteine cytotoxicity compared with undifferentiated cells (He et al., 2013; Zhao et al., 2012). In this study, we have used undifferentiated HT22 cells. Therefore, it is our speculation that differentiation of HT22 cells might enhance αNF-induced cell death through AhR crosstalk with NMDA receptor. It remains to be determined whether differentiation of HT22 cells might change the effects of and mechanisms of αNF on cell death.

c-Src is a cytosolic tyrosine kinase that has been shown to participate in AhR signaling through non-genomic pathway (Dong and Matsumura, 2009; Matsumura, 2009; Tomkiewicz et al., 2013). Because αNF increased phosphorylation and activation of c-Src at Tyr416 (Fig. 6A), we postulated that αNF-induced c-Src may play a role in ER stress and apoptosis. This hypothesis was supported by the observation that treatment with c-Src inhibitor, SU6656, and knockdown of c-Src by siRNA transfection reduced αNF-induced CHOP expression and cell death (Fig. 6B-E). Inhibition of c-Src reduced αNF-induced ROS generation and phosphorylation of MAPKs (Fig. 6F, G), suggesting that c-Src is upstream of ROS and MAPKs in HT22 cells. Further studies are required how αNF activates c-Src.

αNF was shown to act as an AhR antagonist but it also had a partial agonistic activity for AhR (Santostefano et al., 1993). Therefore, we examined the role of AhR in αNF-induced ER stress and apoptosis. Our results showed that αNF did not significantly affect the protein and mRNA expression of AhR itself, whereas it increased the protein and mRNA expression of Cyp1a1 (Fig. 7A), indicating an activation of AhR and subsequent transcriptional expression of AhR-target genes. Involvement of AhR activation was also supported by the fact that inhibition of AhR by an antagonist, CH223191, or reduction of AhR expression by AhR siRNA transfection significantly blocked αNF-induced CHOP expression and cell death in HT22 cells (Fig. 7B-E). Consistently, it was reported that αNF at high concentration (10 μM) has a strong AhR agonist activity for DRE-mediated CYP1 A1 induction in Huh cells (Murray et al., 2011). Moreover, knockdown of ARNT, the heterodimerizing partner of AhR for transcriptional activation, reduced αNF-induced cell death and CHOP expression (Fig. 7G and H). The results suggest that αNF-induced CHOP expression and cell death are ARNT-dependent in HT22 neuronal cells. Taken together, these results imply that αNF shows pro-apoptotic action as an AhR agonist through AhR/ARNT-dependent genomic pathway in HT22 neuronal cells.

To confirm that αNF increases AhR-dependent transcriptional activity in HT22 cells, we examined the relative luciferase activity after transfection of pGL3-DRE-Luc plasmid that contains AhR-responsive element (DRE for CYP1 A1) and luciferase reporter gene. By this experiment, we clearly demonstrated that αNF can induce DRE-luciferase activity (Fig. 8A), suggesting that αNF acts as an AhR agonist in HT22 moue hippocampal neuronal cells. The agonistic effect of αNF was confirmed by the fact that αNF-dependent DRE luciferase activity was reduced in HT22 cells by pretreatment with an AhR antagonist, CH223191, or transfected with AhR and ARNT siRNAs, (Fig. 8A). Because inhibition of MAPKs by MAPK inhibitors or siRNA transfection blocked αNF-induced DRE-luciferase activity (Fig. 8B and C), we suggest that MAPKs might be upstream of AhR-dependent transcriptional activation, ER stress, and cell death. Furthermore, we found that inhibition of c-Src by SU6656 or c-Src siRNA reduced αNF-induced DRE luciferase activity (Fig. 8D) and Cyp1a1 mRNA expression (Fig. 8E and F). In contrast to other reports of c-Src-mediated inflammatory responses through a non-genomic pathway (Matsumura, 2009; Tomkiewicz et al., 2013; Xie et al., 2012), our results suggest that c-Src may mediate αNF-induced apoptosis and ER stress, at least partially, through AhR- and ARNT-dependent genomic pathway. However, the possibility of involvement of non-genomic pathways could not be excluded at this moment. Further experiments are needed to clarify it.

In summary, we found that αNF induced apoptotic cell death through ER stress in HT22 hippocampal neuronal cells. αNF induced apoptosis and ER stress via c-Src-, ROS-, MAPKs-, and AhR/ARNT-dependent pathways in these cells. Moreover, αNF induced cell death and ER stress through AhR/ARNT-dependent genomic pathway (Fig. 9). Further studies are necessary to determine the pro-apoptotic effects of AhR ligands and molecular mechanisms involved in brain damage using an *in vivo* animal model.

## Conflict of interest

No conflict of interest is declared.

## Acknowledgements

This work was supported by the National Research Foundation of Korea (NRF) grants funded by the Korea government (No. 2018R1A2B6004356; 2018R1A6A1A03025124) and a grant of the Korea Health Technology R&D Project through the Korea Health Industry Development Institute (KHIDI) funded by the Ministry of Health & Welfare, Republic of Korea (No. HI14C2700).

## References

Aires, V., Hichami, A., Filomenko, R., Ple, A., Rebe, C., Bettaieb, A., Khan, N.A., 2007. Docosahexaenoic acid induces increases in [Ca2 + ]i via inositol 1,4,5-triphosphate production and activates protein kinase C gamma and -delta via phosphatidylserine binding site: implication in apoptosis in U937 cells. Mol. Pharmacol. 72 (6), 1545–1556.

Backlund, M., Ingelman-Sundberg, M., 2005. Regulation of aryl hydrocarbon receptor signal transduction by protein tyrosine kinases. Cell. Signal. 17 (1), 39–48.

Barouki, R., Coumoul, X., Fernandez-Salguero, P.M., 2007. The aryl hydrocarbon receptor, more than a xenobiotic-interacting protein. FEBS Lett. 581 (19), 3608–3615.
Bock, K.W., 2016. Toward elucidation of dioxin-mediated chloracne and Ah receptor functions. Biochem. Pharmacol. 112, 1–5.
Boyce, M., Bryant, K.F., Jousse, C., Long, K., Harding, H.P., Scheuner, D., Kaufman, R.J., Ma, D., Coen, D.M., Ron, D., Yuan, J., 2005. A selective inhibitor of eIF2alpha dephosphorylation protects cells from ER stress. Science 307 (5711), 935–939.
Boyce, M., Yuan, J., 2006. Cellular response to endoplasmic reticulum stress: a matter of life or death. Cell Death Differ. 13 (3), 363–373.
Butler, R.A., Kelley, M.L., Olberding, K.E., Gardner, G.R., Van Beneden, R.J., 2004. Aryl hydrocarbon receptor (AhR)-independent effects of 2,3,7,8-tetrachlorodibenzo-p-dioxin (TCDD) on softshell clam (Mya arenaria) reproductive tissue. Comp. Biochem. Physiol. C Toxicol. Pharmacol. 138 (3), 375–381.
Cheng, Y.W., Li, C.H., Lee, C.C., Kang, J.J., 2003. Alpha-naphthoflavone induces vasorelaxation through the induction of extracellular calcium influx and NO formation in endothelium. Naunyn Schmiedebergs Arch. Pharmacol. 368 (5), 377–385.
Chepelev, N.L., Moffat, I.D., Bowers, W.J., Yauk, C.L., 2015. Neurotoxicity may be an overlooked consequence of benzo[a]pyrene exposure that is relevant to human health risk assessment. Mutat. Res. Rev. Mutat. Res. 764, 64–89.
Choi, A.Y., Choi, J.H., Lee, J.Y., Yoon, K.S., Choe, W., Ha, J., Yeo, E.J., Kang, I., 2010. Apigenin protects HT22 murine hippocampal neuronal cells against endoplasmic reticulum stress-induced apoptosis. Neurochem. Int. 57 (2), 143–152.
Choi, A.Y., Choi, J.H., Yoon, H., Hwang, K.Y., Noh, M.H., Choe, W., Yoon, K.S., Ha, J., Yeo, E.J., Kang, I., 2011. Luteolin induces apoptosis through endoplasmic reticulum stress and mitochondrial dysfunction in Neuro-2a mouse neuroblastoma cells. Eur. J. Pharmacol. 668 (1-2), 115–126.
Choi, J.H., Jeong, Y.J., Yu, A.R., Yoon, K.S., Choe, W., Ha, J., Kim, S.S., Yeo, E.J., Kang, I., 2017. Fluoxetine induces apoptosis through endoplasmic reticulum stress via mitogen-activated protein kinase activation and histone hyperacetylation in SK-N-BE (2)-M17 human neuroblastoma cells. Apoptosis 22 (9), 1079–1097.
Chopra, M., Schrenk, D., 2011. Dioxin toxicity, aryl hydrocarbon receptor signaling, and apoptosis-persistent pollutants affect programmed cell death. Crit. Rev. Toxicol. 41 (4), 292–320.
Cuartero, M.I., Ballesteros, I., de la Parra, J., Harkin, A.L., Abautret-Daly, A., Sherwin, E., Fernandez-Salguero, P., Corbi, A.L., Lizasoain, I., Moro, M.A., 2014. L-kynurenine/aryl hydrocarbon receptor pathway mediates brain damage after experimental stroke. Circulation 130 (23), 2040–2051.
Datta, A., Bhasin, N., Kim, H., Ranjan, M., Rider, B., Abd Elmageed, Z.Y., Mondal, D., Agrawal, K.C., Abdel-Mageed, A.B., 2015. Selective targeting of FAK-Pyk2 axis by alpha-naphthoflavone abrogates doxorubicin resistance in breast cancer cells. Cancer Lett. 362 (1), 25–35.
Denison, M.S., Nagy, S.R., 2003. Activation of the aryl hydrocarbon receptor by structurally diverse exogenous and endogenous chemicals. Annu. Rev. Pharmacol. Toxicol. 43, 309–334.
Dong, B., Matsumura, F., 2009. The conversion of rapid TCCD nongenomic signals to persistent inflammatory effects via select protein kinases in MCF10A cells. Mol. Endocrinol. 23 (4), 549–558.
Duan, Z., Zhao, J., Fan, X., Tang, C., Liang, L., Nie, X., Liu, J., Wu, Q., Xu, G., 2014. The PERK-eIF2alpha signaling pathway is involved in TCDD-induced ER stress in PC12 cells. Neurotoxicology 44, 149–159.
Flores-Perez, A., Elizondo, G., 2018. Apoptosis induction and inhibition of HeLa cell proliferation by alpha-naphthoflavone and resveratrol are aryl hydrocarbon receptor-independent. Chem. Biol. Interact. 281, 98–105.
Furness, S.G., Whelan, F., 2009. The pleiotropy of dioxin toxicity–xenobiotic misappropriation of the aryl hydrocarbon receptor's alternative physiological roles. Pharmacol. Ther. 124 (3), 336–353.
Gordeeva, A.V., Zvyagilskaya, R.A., Labas, Y.A., 2003. Cross-talk between reactive oxygen species and calcium in living cells. Biochem. Mosc. 68 (10), 1077–1080.
He, M., Liu, J., Cheng, S., Xing, Y., Suo, W.Z., 2013. Differentiation renders susceptibility to excitotoxicity in HT22 neurons. Neural Regen. Res. 8 (14), 1297–1306.
Henklova, P., Vrzal, R., Ulrichova, J., Dvorak, Z., 2008. Role of mitogen-activated protein kinases in aryl hydrocarbon receptor signaling. Chem. Biol. Interact. 172 (2), 93–104.
Hsiao, G., Chang, C.Y., Shen, M.Y., Chou, D.S., Tzeng, S.H., Chen, T.F., Sheu, J.R., 2005. alpha-Naphthoflavone, a potent antiplatelet flavonoid, is mediated through inhibition of phospholipase C activity and stimulation of cyclic GMP formation. J. Agric. Food Chem. 53 (13), 5179–5186.
Jeon, Y.J., Youk, E.S., Lee, S.H., Suh, J., Na, Y.J., Kim, H.M., 2002. Polychlorinated biphenyl-induced apoptosis of murine spleen cells is aryl hydrocarbon receptor independent but caspases dependent. Toxicol. Appl. Pharmacol. 181 (2), 69–78.
Kajta, M., Wojtowicz, A.K., Mackowiak, M., Lason, W., 2009. Aryl hydrocarbon receptor-mediated apoptosis of neuronal cells: a possible interaction with estrogen receptor signaling. Neuroscience 158 (2), 811–822.
Kakeyama, M., Tohyama, C., 2003. Developmental neurotoxicity of dioxin and its related compounds. Ind. Health 41 (3), 215–230.
Kaufman, R.J., 1999. Stress signaling from the lumen of the endoplasmic reticulum: coordination of gene transcriptional and translational controls. Genes Dev. 13 (10), 1211–1233.
Lee, Y.C., Oslund, K.L., Thai, P., Velichko, S., Fujisawa, T., Duong, T., Denison, M.S., Wu, R., 2011. 2,3,7,8-Tetrachlorodibenzo-p-dioxin-induced MUC5AC expression: aryl hydrocarbon receptor-independent/EGFR/ERK/p38-dependent SP1-based transcription. Am. J. Respir. Cell Mol. Biol. 45 (2), 270–276.
Liao, P.L., Li, C.H., Chang, C.Y., Lu, S.R., Lin, C.H., Tse, L.S., Cheng, Y.W., 2012. Anti-ageing effects of alpha-naphthoflavone on normal and UVB-irradiated human skin fibroblasts. Exp. Dermatol. 21 (7), 546–548.
Lin, C.H., Chen, C.C., Chou, C.M., Wang, C.Y., Hung, C.C., Chen, J.Y., Chang, H.W., Chen, Y.C., Yeh, G.C., Lee, Y.H., 2009. Knockdown of the aryl hydrocarbon receptor attenuates excitotoxicity and enhances NMDA-induced BDNF expression in cortical neurons. J. Neurochem. 111 (3), 777–789.
Lin, C.H., Juan, S.H., Wang, C.Y., Sun, Y.Y., Chou, C.M., Chang, S.F., Hu, S.Y., Lee, W.S., Lee, Y.H., 2008. Neuronal activity enhances aryl hydrocarbon receptor-mediated gene expression and dioxin neurotoxicity in cortical neurons. J. Neurochem. 104 (5), 1415–1429.
Lindholm, D., Wootz, H., Korhonen, L., 2006. ER stress and neurodegenerative diseases. Cell Death Differ. 13 (3), 385–392.
Matsumura, F., 2009. The significance of the nongenomic pathway in mediating inflammatory signaling of the dioxin-activated Ah receptor to cause toxic effects. Biochem. Pharmacol. 77 (4), 608–626.
Mense, S.M., Singh, B., Remotti, F., Liu, X., Bhat, H.K., 2009. Vitamin C and alpha-naphthoflavone prevent estrogen-induced mammary tumors and decrease oxidative stress in female ACI rats. Carcinogenesis 30 (7), 1202–1208.
Morales-Hernandez, A., Corrales-Redondo, M., Marcos-Merino, J.M., Gonzalez-Rico, F.J., Sanchez-Martin, F.J., Merino, J.M., 2016. AhR-dependent 2,3,7,8-tetrachlorodibenzo-p-dioxin toxicity in human neuronal cell line SHSY5Y. Neurotoxicology 56, 55–63.
Morales-Hernandez, A., Sanchez-Martin, F.J., Hortigon-Vinagre, M.P., Henao, F., Merino, J.M., 2012. 2,3,7,8-Tetrachlorodibenzo-p-dioxin induces apoptosis by disruption of intracellular calcium homeostasis in human neuronal cell line SHSY5Y. Apoptosis 17 (11), 1170–1181.
Murray, I.A., Flaveny, C.A., Chiaro, C.R., Sharma, A.K., Tanos, R.S., Schroeder, J.C., Amin, S.G., Bisson, W.H., Kolluri, S.K., Perdew, G.H., 2011. Suppression of cytokine-mediated complement factor gene expression through selective activation of the Ah receptor with 3',4'-dimethoxy-alpha-naphthoflavone. Mol. Pharmacol. 79 (3), 508–519.
Murray, I.A., Patterson, A.D., Perdew, G.H., 2014. Aryl hydrocarbon receptor ligands in cancer: friend and foe. Nat. Rev. Cancer 14 (12), 801–814.
Nishijo, M., Kuriwaki, J., Hori, E., Tawara, K., Nakagawa, H., Nishijo, H., 2007. Effects of maternal exposure to 2,3,7,8-tetrachlorodibenzo-p-dioxin on fetal brain growth and motor and behavioral development in offspring rats. Toxicol. Lett. 173 (1), 41–47.
Opitz, C.A., Litzenburger, U.M., Sahm, F., Ott, M., Tritschler, I., Trump, S., Schumacher, T., Jestaedt, L., Schrenk, D., Weller, M., Jugold, M., Guillemin, G.J., Miller, C.L., Lutz, C., Radlwimmer, B., Lehmann, I., von Deimling, A., Wick, W., Platten, M., 2011. An endogenous tumour-promoting ligand of the human aryl hydrocarbon receptor. Nature 478 (7368), 197–203.
Park, W.H., Jun, D.W., Kim, J.T., Jeong, J.H., Park, H., Chang, Y.S., Park, K.S., Lee, H.K., Pak, Y.K., 2013. Novel cell-based assay reveals associations of circulating serum AhR-ligands with metabolic syndrome and mitochondrial dysfunction. Biofactors 39 (4), 494–504.
Puga, A., Ma, C., Marlowe, J.L., 2009. The aryl hydrocarbon receptor cross-talks with multiple signal transduction pathways. Biochem. Pharmacol. 77 (4), 713–722.
Rao, V.R., Finkbeiner, S., 2007. NMDA and AMPA receptors: old channels, new tricks. Trends Neurosci. 30 (6), 284–291.
Sanchez-Martin, F.J., Fernandez-Salguero, P.M., Merino, J.M., 2011. Aryl hydrocarbon receptor-dependent induction of apoptosis by 2,3,7,8-tetrachlorodibenzo-p-dioxin in cerebellar granule cells from mouse. J. Neurochem. 118 (1), 153–162.
Santostefano, M., Merchant, M., Arellano, L., Morrison, V., Denison, M.S., Safe, S., 1993. Alpha-Naphthoflavone-induced CYP1A1 gene expression and cytosolic aryl hydrocarbon receptor transformation. Mol. Pharmacol. 43 (2), 200–206.
Song, Z., Pollenz, R.S., 2002. Ligand-dependent and independent modulation of aryl hydrocarbon receptor localization, degradation, and gene regulation. Mol. Pharmacol. 62 (4), 806–816.
Tomkiewicz, C., Herry, L., Bui, L.C., Metayer, C., Bourdeloux, M., Barouki, R., Coumoul, X., 2013. The aryl hydrocarbon receptor regulates focal adhesion sites through a non-genomic FAK/Src pathway. Oncogene 32 (14), 1811–1820.
Wang, H.C., Zhou, Y., Huang, S.K., 2017. SHP-2 phosphatase controls aryl hydrocarbon receptor-mediated ER stress response in mast cells. Arch. Toxicol. 91 (4), 1739–1748.
Williamson, M.A., Gasiewicz, T.A., Opanashuk, L.A., 2005. Aryl hydrocarbon receptor expression and activity in cerebellar granule neuroblasts: implications for development and dioxin neurotoxicity. Toxicol. Sci. 83 (2), 340–348.
Xie, G., Peng, Z., Raufman, J.P., 2012. Src-mediated aryl hydrocarbon and epidermal growth factor receptor cross talk stimulates colon cancer cell proliferation. Am. J. Physiol. Gastrointest. Liver Physiol. 302 (9), G1006–1015.
Yoshioka, H., Hiromori, Y., Aoki, A., Kimura, T., Fujii-Kuriyama, Y., Nagase, H., Nakanishi, T., 2012. Possible aryl hydrocarbon receptor-independent pathway of 2,3,7,8-tetrachlorodibenzo-p-dioxin-induced antiproliferative response in human breast cancer cells. Toxicol. Lett. 211 (3), 257–265.
Zhao, Z., Lu, R., Zhang, B., Shen, J., Yang, L., Xiao, S., Liu, J., Suo, W.Z., 2012. Differentiation of HT22 neurons induces expression of NMDA receptor that mediates homocysteine cytotoxicity. Neurol. Res. 34 (1), 38–43.
Zhu, Y., Bi, F., Li, Y., Yin, H., Deng, N., Pan, H., Li, D., Xiao, B., 2017. Alpha- and beta-naphthoflavone synergistically attenuate H2O2-induced neuron SH-SY5Y cell damage. Exp. Ther. Med. 13 (3), 1143–1150.
Zinszner, H., Kuroda, M., Wang, X., Batchvarova, N., Lightfoot, R.T., Remotti, H., Stevens, J.L., Ron, D., 1998. CHOP is implicated in programmed cell death in response to impaired function of the endoplasmic reticulum. Genes Dev. 12 (7), 982–995.